www.vbripress.com, www.amlett.com, DOI: 10.5185/amlett.2010.12192 Published online by the VBRI press in 2011

Effect of KBF_4 and K_2TiF_6 on precipitation kinetics of TiB_2 in aluminium matrix composite

N.B. Dhokey, S. Ghule, K. Rane, R.S. Ranade

Department of Metallurgical Engineering, Govt. College of Engineering Pune 411005, India

*Corresponding author. Tel: (+91) 20 25507262; E-mail: nbdhokey@yahoo.co.in

Received: 14 Dec 2010, Revised: 24 Feb 2011 and Accepted: 01 March 2011

ABSTRACT

Aluminium reinforced with TiB_2 is an emerging class of metal matrix composites for many engineering applications such as automobiles, aerospace and naval vessels. The initial part of the present work study involves melting of individual fluxes of KBF_4 and $KTiF_6$ in premelted aluminium in an induction furnace. In the later part of the work covers the combined effect of these fluxes to produce aluminium metal matrix composites containing 2.5% TiB_2. The effect of the varying amount of KBF_4 on kinetics of TiB_2 formation and elimination other unstable phases was studied. The material was examined for hardness, microstructures and wear rates using Pin-on-Disc test machine, XRD and SEM-EDX analysis. The effect of TiB_2 on properties was analysed. It was concluded that an optimum level of KBF_4 is needed to get critical population of TiB_2 particles in the matrix. Copyright © 2011 VBRI press.

Keywords: Metal matrix composites; XRD; SEM-EDX.

Narendra B Dhokey received Ph.D. from V.N.I.T Nagpur in 2007 and M. Tech. (Process Metallurgy) in 1995 from I.I.T.Mumbai. Presently he is working as Professor in Department of Metallurgical Engineering, Govt. College of Engineering Pune (India). He has published more than 40 papers in National and International Journal and conferences. He has 20 years of teaching experience including 6 years industrial experience in Steel plant. His main area of research is Synthesis of alloys, Powder Metallurgy, Cryogenic treatment of materials and Tribology of materials.

K. K. Rane perusing M. Tech. in Process Metallurgy from Department of Metallurgy and Materials Science, Government College of Engineering, Pune. He obtained B.E. in Mechanical Engineering from North Maharashtra University, India in 2009. Presently, he is working as Project Fellow on UGC project in Metallurgy and Material Science Department, College of Engineering, Pune. His main research areas are advance casting techniques, wear, metal matrix composites and ceramic engineering.

Introduction

Composite materials on aluminium alloy matrices are manufactured by powder metallurgy, applying the mechanical alloying process, co-spray deposition process of dispersion particles in atomised aluminium alloys as well as by squeeze casting methods. The mechanical properties of composite materials reinforced with ceramic particles depend on the matrix properties, mutual wettability at interphase and the amount of reinforcing phase and the diameter of the reinforcing particles. The advantages of composite materials are high resistance to wear, good strength, and relatively good heat conduction, resulted in their practical application as brake disc of car [**1**].

Aluminium-based reinforced TiB_2 exhibits improved mechanical and corrosion properties which find relevance in automobiles and aerospace materials for structural applications and also in naval vessels [**2**]. A review on Al-Ti-B ternary system indicated that very small amounts of Ti (0.005 wt.%) and B (0.001 wt.%) in liquid Al have a remarkable grain refining effect [**3**]. Aluminium TiB_2 composite has been made using mixed salts of potassium hexafluorotitanate (K_2TiF_6) and potassium tetrafluororate (KBF_4) in stirred aluminium melt [**4**]. In-situ Al-7Si/TiB_2 particulate composites show significant improvement in hardness, yield strength, tensile strength, Young's modulus and wear resistance. It also confirms that the diborides AlB_2 and TiB_2 do not form a continuous solid solution and AlB_2 forms through a peritectic reaction between AlB_{12} and liquid at 1030°C [**5**]. Transformation mechanism of $TiAl_3$ to TiB_2 revealed that size of $TiAl_3$ particles is quite larger than TiB_2 particles [**6, 7**]. Thermodynamic model for describing the formation of in-situ TiB_2 reinforced Al metal matrix composite (MMC) has been proposed [**8**]. An attempt on thermodynamic analysis on the formation of in-situ reinforced phases TiB_2+Al_3Ti in Al-4.5Cu composites was investigated by mixed salts reaction with an addition of Na_3AlF_6 to facilitate the kinetics of the reaction[**9**]. In situ Al- TiB_2 composites were synthesized successfully through the mixing salts reaction among the KBF_4, K_2TiF_6 and Al. The agglomerations (clusters) of the particles distribute uniformly in the Al matrix. The TiB_2 particles are hexangular and near-equiaxed shape. The average size of TiB_2 particle is about 1 μm [**10**]. Dispersion strengthening takes place by nano-scale TiB_2 particles, increases the mechanical properties of metal matrix composite due to improved interfacial strength. Crack initiation in tensile specimens is preferred at particles; however, the presence of TiB_2 nano particles reduces ductility of the in situ composite [**11**]. There is limited solubility of Aluminium in TiB_2 and Titanium in AlB_2 exist, hence a continuous compound (Al, Ti)B_2 is not stable [**12**].Aluminium with TiB_2 Reinforcement has a higher tensile strength than pure Aluminium alloy with reduced ductility. The significant improvement in the mechanical properties of the composite when compared with the Aluminium alloy can be attributed to the distribution of TiB_2 particles in the matrix [**13**]. In the present research work, systematic effort is made to produce Aluminium-based TiB_2 composite by optimising content of KBF_4.

Experimental

Materials and fabrication

In-situ Aluminium-TiB_2 composite was produced using fluxes of potassium hexafluorotitanate (K_2TiF_6, make: Fluka Analytical) and potassium tetrafluororate (KBF_4 make: Aldrich). A few experiments, as given in Table 4.1, were conducted by allowing melting of individual fluxes (KBF_4 and K_2TiF_6) in aluminium in accordance with equations (1, 2). In the subsequent experiments as per equation (3), the combined effect of two fluxes was attempted in aluminium melted in Induction furnace (25KW, make Autocontrol, Mumbai). The corresponding reactions can be stated as-

$$3K_2TiF_6 + 13Al \rightarrow 3TiAl_3 + 3KAlF_4 + K_3AlF_6 \quad \text{............... (1)}$$

$$2KBF_4 + 3Al \rightarrow AlB_2 + 2KAlF_4 \quad \text{............... (2)}$$

Net reaction,

$$K_2TiF_6 + 2KBF_4 + (22/3)\ Al \rightarrow TiAl_3 + AlB_2 + 3KAlF_4 + (1/3)\ K_3AlF_6 \quad \text{............... (3)}$$

$$AlB_2 + TiAl_3 \rightarrow TiB_2 + 4Al \quad \text{............... (4)}$$

Material characterization

Metallography: Electrolytic etching and polishing machine is used for sample preparation. Electrolytic bath used consisted of Methanol-730 ml, Butyl Cellosolve-98 ml, Perchloric acid-78 ml and distilled water-100 ml. Microstructural analysis was carried out with the help of inverted microscope [make-CARL ZEISS Germany, model-Axiovert 40Mat]. SEM photographs were obtained using Scanning Electron Microscope (make-Joel, Japan). EDS was carried out for localised chemical analysis of particular phases. For XRD (Philips Analytical) analysis, a plot of 2-theta verses intensity could be analysed using Origin Plus software and phase identification done by High Score Plus software.

Microhardness measurement: The hardness of each sample after treatment was measured by using Micro Hardness machine (FM -700, make: Future- tech). The load applied was 100 gram with dwell time of 15 seconds. For each sample, average of five reading was reported.

Wear loss measurement: Pin-on-Disc wear test machine (M/s Magnum Engineers, Bangalore) was used for wear analysis. Wear test specimen of 10 mm dia. was subjected to sliding speed of 1.2 m/s and an applied load of 6 kg for a sliding distance of 3000 m. During testing, the pin specimen was kept stationary perpendicular to disc while the circular disc was rotated. The apparatus had a pin of SAE 52100 steel (RC 61) and 0.3 μRa surface roughness disc of diameter 170 mm was used as counter face disc.

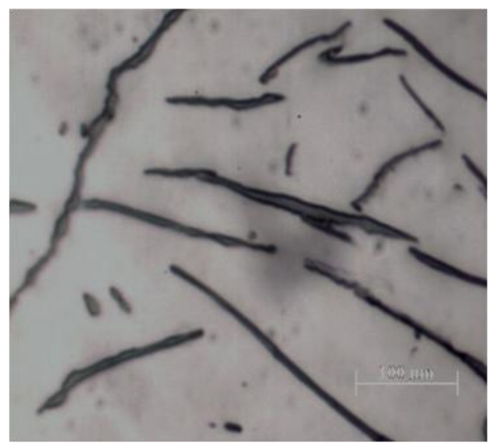

Fig. 1. Microstructure showing flakes of Al_3Ti in matrix of alumnium Expt. 2.

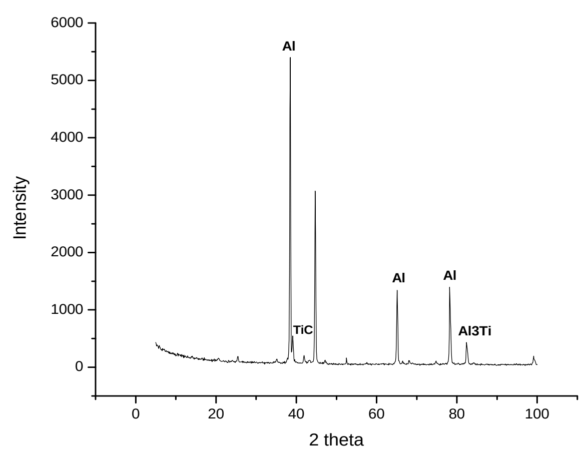

Fig. 2. XRD pattern reveals peaks of Al_3Ti, Al and TiC of Expt. 2.

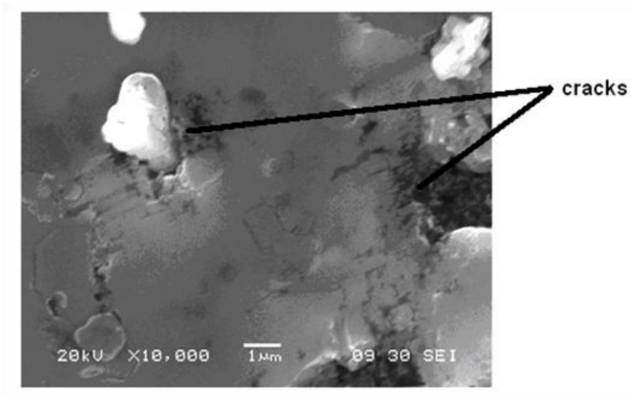

Fig. 3. SEM micrographs, magnified view of Al_3Ti flake of Fig.1, showing several fine cracks on surface of Al_3Ti phase of Expt. 2.

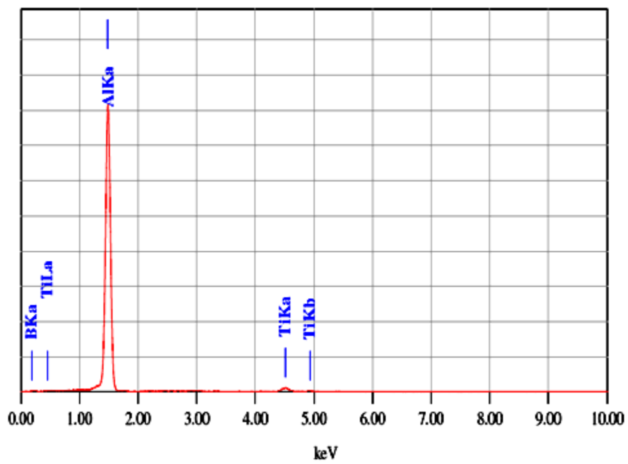

Fig. 4. EDS spot analysis of Al_3Ti phase of Fig. 3 to quantify elements (Expt. 2).

Fig. 5. Microstructure of precipitates of AlB_2 in alumnium matrix (Expt. 3).

Results

Effect of K_2TiF_6 on aluminium

Fig. 1 shows flakes of Al_3Ti in the matrix of pure aluminium. These precipitates of Al_3Ti were confirmed by XRD analysis as indicated in **Fig. 2**. Further SEM analysis of Al_3Ti phase was analysed to reveal surface topography which indicates numerous fine cracks as depicted in **Fig. 3**. Similar features have been noted by other researchers [**5**]. The presence of Al_3Ti was further reconfirmed using SEM-EDS as shown in **Fig. 4**. The chemical reaction of aluminium with K_2TiF_6 is governed by equation (1).

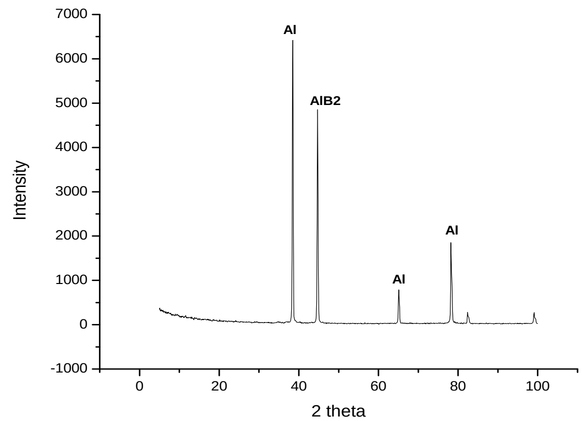

Fig. 6. XRD pattern clearly showing AlB_2 phase (Expt. 3).

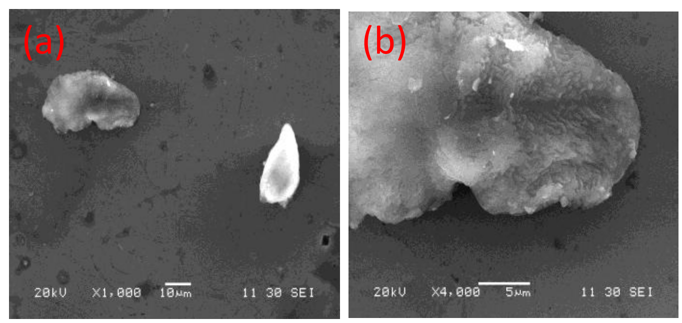

Fig. 7. SEM micrographs showing AlB_2 particles in Al matrix at (a) X1000 and (b) X4000 magnifications.

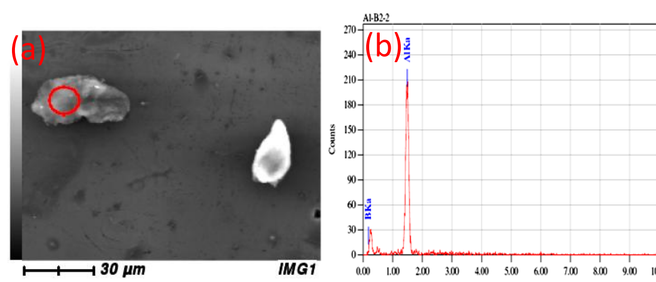

Fig. 8. EDX spectrum and elemental mapping of AlB_2 particle in Aluminium matrix clearly showing boron rich phase (Expt. 3).

Effect of KBF_4 on aluminium

Fig. 5 shows uniform distribution of AlB_2 phase which is having rod like morphology [**5**]. The chemical reaction of KBF_4 with Aluminium is governed by equation (2). It is further quantified by XRD as shown in **Fig. 6**. Surface topography of the phase is shown in **Fig. 7**, however some roughness is seen on AlB_2 precipitate. Elemental mapping of TiB_2 is in **Fig. 8**.

Recoveries of titanium and boron

This study was required to find whether stoichiometry calculation is enough to complete the reaction to get maximum percent TiB_2 or whether any additional reactant species particularly KBF_4 is needed in excess than stoichiometry. It is observed from chemical analysis of few experiments that there is an average 86.61% Titanium recovery and 34.76% boron recovery, similar level of recovery values have been reported in published work [**9**].

This implies that around 13 % Titanium and 65% Boron lost to slag for various reactions in the form of some allied phases in slag and some may be in the form of gaseous products. In view of the facts, the corrective actions were taken in subsequent experiments to add excess amount of KBF_4 over and above the stoichiometry. Based on the analysis, few experiments (Expts. 5 and 6) were conducted using 120% and 140% KBF_4.

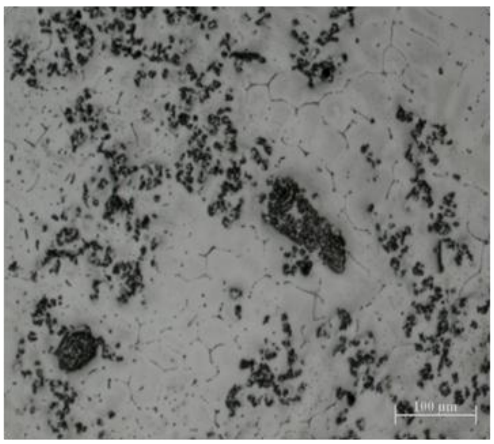

Fig. 9. Optical microstructure showing isolated pockets of TiB_2 and some flakes of Al_3Ti (Expt. 4).

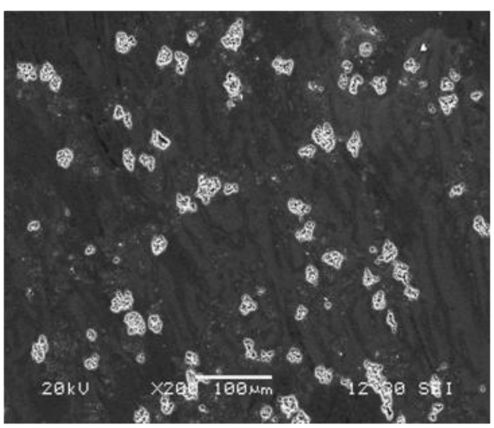

Fig. 10. SEM micrographs showing uniformly precipitated reaction products in Al matrix (Expt. 4).

Variation of KBF_4 on combined melting of fluxes

Microstructure Al-TiB_2 composites taken by optical microscopy is shown in **Fig. 9**. The segregated pockets of TiB_2 and Al_3Ti are clearly seen at isolated location. It is difficult to say about the size and shape of TiB_2 particles due to its ultrafine nature of TiB_2. Hence SEM was used to estimate the size of the TiB_2. SEM analysis was conducted to investigate morphological features of TiB_2 particles. As revealed from **Fig. 10** that these TiB_2 particles are moderately distributed in the Al matrix. It is evident from SEM analysis that TiB_2 particles are very fine in size, typically 1 µm and brilliant white in color (**Fig. 11**). It is possible that TiB_2 nucleation takes place in $AlTi_3$ phase which has been quantitatively analyzed by SEM-EDS in **Fig. 12**. In aluminium matrix, there are traces of B and Ti as depicted in **Fig. 13**.

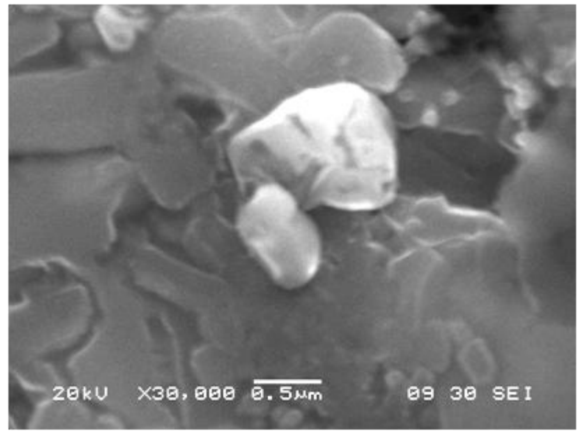

Fig. 11. SEM micrographs showing TiB_2 particles in Al matrix depicting size of TiB_2 less than 1 µm (Expt. 4).

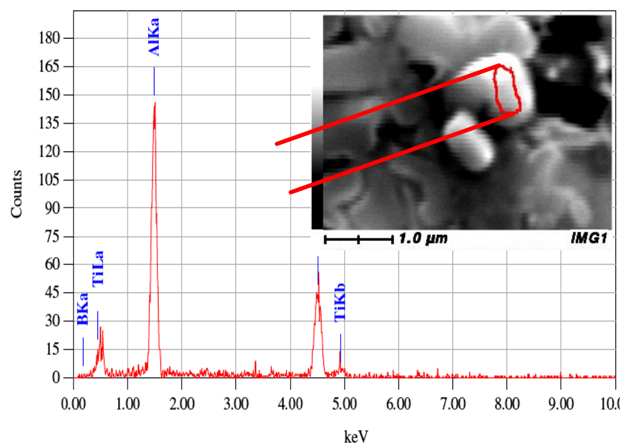

Fig.12. EDX spectrum of TiB_2 precipitates as seen in inset and elemental mapping of TiB_2 particle (Expt. 4).

Identification of phases

Fig. 14 shows the XRD pattern of Al based TiB_2 composite indicates presence of TiB_2 along with Al_3Ti. This experiment was carried out strictly as per stoichiometry and its XRD analysis reveals presence of intermediate unstable phase like Al_3Ti. It evident that there is a shortage of Boron towards completeness of the reaction for achieving complete conversion to TiB_2 precipitates. Hence in subsequent experiment excess amount to the tune of 120%KBF_4 was added and it is seen that there is elimination of extra peak of Al_3Ti phase as shown in **Fig. 15**.

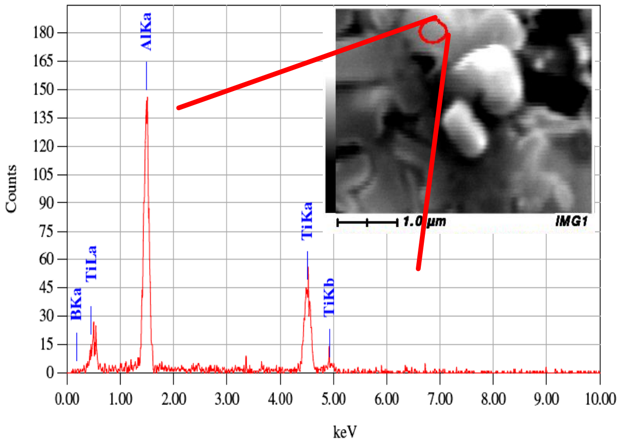

Fig. 13. EDX spectrum and elemental mapping of matrix showing in inset p Aluminium and traces of B and Ti dissolved in aluminium matrix Expt. 4.

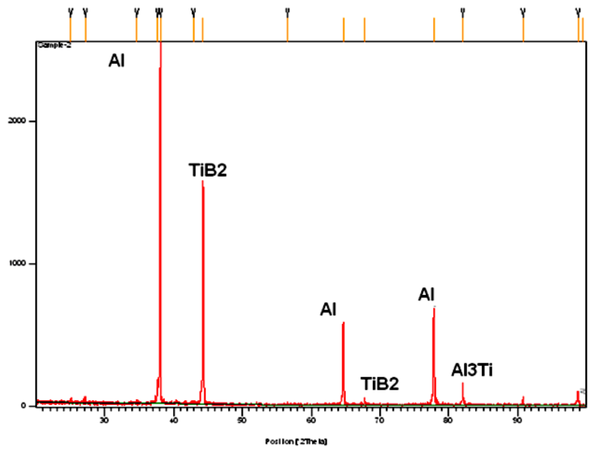

Fig. 14. XRD pattern of Al-2.5%TiB_2, 100% stoichiometry (Expt. 4).

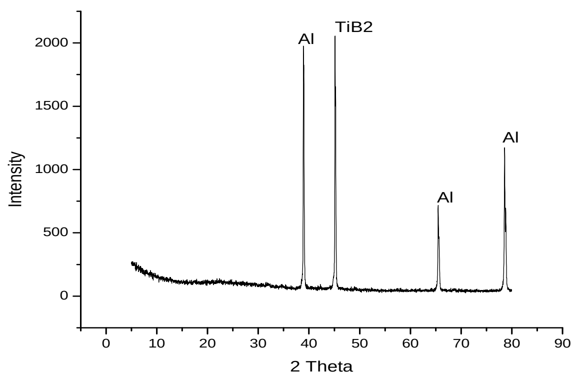

Fig. 15. XRD pattern clearly showing TiB_2 phase in Aluminium matrix (120% KBF_4) Expt. 5.

Discussion

Mechanism of TiB_2 precipitation

In accordance to the chemical reactions given by Equations 1, 2, 3 and 4, it is obvious that $AlTi_3$ and AlB_2 unstable phases are formed even though both the halide fluxes K_2TiF_6 and KBF_4 are added simultaneously. The morphology of these unstable phases is quite distinct as depicted in **Fig. 1** and **5**. The first step involves the formation of $AlTi_3$ phase along with AlB_2. When these phases come in intimate contact, then migration of Ti and B starts. The nucleation of TiB_2 takes place in $AlTi_3$ phase with regeneration of Aluminium during this process [**14**]. Boron diffusion to $AlTi_3$ is sluggish and hence it necessitates the additional quantity of KBF_4 requires to be added up beyond the stoichiometry to enhance the kinetics of precipitation of TiB_2. Overall boron migration is the rate controlling mechanism.

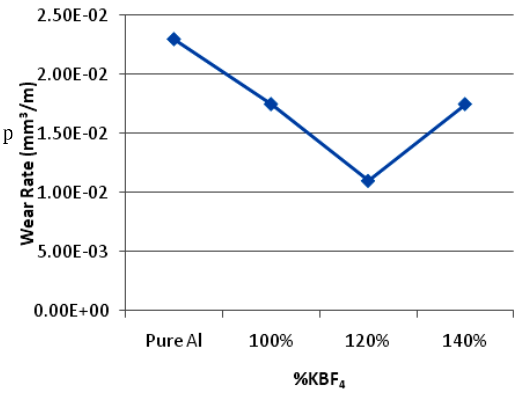

Fig. 16. Variation of KBF_4 on wear rate of Al-2.5%TiB_2 composites and its comparison with pure aluminium.

Table 1. Description of experiments conducted in induction furnace.

Expt. No.	Description of material
1.	Pure Aluminium (Al)
2.	Al + $KTiF_6$
3.	Al + KBF_4
4.	Al +2.5%TiB_2 (Stoichiometric addition of KBF_4 and $KTiF_6$)
5.	Al +2.5%TiB_2 (120%KBF_4, excess than stoichiometry)
6.	Al +2.5%TiB_2 (140%KBF_4, excess than stoichiometry)

Table 2. Micro hardness (Load=100 gram, Dwell Time=15 sec) of cast materials of various experiments.

Expt. No.	Description of material	Avg. Micro hardness (HV)
1.	Pure Al	27
2.	Pure aluminium + K_2TiF_6	30
3.	Pure aluminium + KBF_4	29
4.	Al-2.5%TiB_2 (Stoichiometric addition of KBF_4 and K_2TiF_6)	34
5.	Al-2.5%TiB_2 (120%KBF_4, excess than stoichiometry)	65
6.	Al-2.5%TiB_2 (140%KBF_4, excess than stoichiometry)	69

Strengthening and microstructural analysis

The increase in hardness in Expt. 4, in which KBF_4 and K_2TiF_6 was added by stoichiometry, show some degree of improvement as evident from **Table 2** over other Expts. 1, 2 and 3. In these composites, not only TiB_2 precipitates are present but also other unstable phases like Al_3Ti (Expt.2) and AlB_2 (Expt.3) are seen. These unstable phases formed with rough surface topography are brittle in nature and are prone to decrease the wear resistance of the sliding material. By increasing content of KBF_4 in Expts.4,5 and 6 showed gradual elimination of these unstable phases. This has a direct bearing on increase in hardness and wear resistance too except in Expt.6. The hardness of the composites increases with increasing TiB_2 content in the aluminium. EDS analysis as shown in **Fig. 13** indicates some degree of solubility of Ti and B in aluminium matrix which is attributed to partial strengthening by way of solid solution.

Wear behaviour

Fig. 16 show the wear rates for pure Aluminium and Al–TiB_2 MMCs for wear test plan of sliding speed of 1.2 m/sec and load of 6 kg. The wear rate of the composites was found to be less than that of pure aluminium. It is observed that lowest wear rate is noted in which 120% KBF_4 is added than stoichiometry. However, the performance is deteriorated in which 140% KBF_4 is added than stoichiometry. It is found that composite with 120% KBF_4 addition gives lower level of wear rate whereas wear rate is more in experiments in which KBF_4 was added 140% above stoichiometry. It means that TiB_2 is stable hard phase which acts as load transfer element. The increase in wear rate is observed for composite in which140%KBF_4 is added with consequent increase in microhardness which might results due to segregation of TiB_2 particles.

Conclusion

Based on the earlier discussion, the following conclusions can be drawn:

- Al-TiB_2 composite (2.5% TiB_2) shows good improvement in hardness as compared to pure Aluminium. It is observed that excess amount to the tune of 120% KBF_4 is required to get optimal level of TiB_2. This fact could be corroborated by the minimum wear rate. Any additional increase to 140%KBF_4, increases hardness but increases wear rate due to weakening of matrix as a result of segregation of TiB_2 particles.
- TiB_2 particles are moderately distributed in Aluminium matrix and are clearly visible in SEM micrographs. The size of TiB_2 particles is about 1µm.

Acknowledgement

The authors thank the University Grant Commission India for providing financial support for this research. Thanks and appreciations are also extended to the Director, College of Engineering, Pune and Dr. P.R. Khangonkar for his valuable inputs and VNIT Nagpur for providing SEM and XRD facility.

Reference

1. Kaczmar, J.W.; Pietrzak, K.; Woosinaski, W. *J. Materials Processing Tech*. **2000**, *106*, 58.
2. Christy, T.V.; Murugan, N.; Kumar, S. *J. Minerals Mat. Char. Engg*. **2010**, *9*, 57. Raghavan,V. *ASM International.* **2005**, *26*,173. **DOI:** 10.1007/s11669-005-0138-9
3. Tjong, S.C.; Ma, Z.Y.; *J. Mat. Sci. Engg*. **2000,** 49. **DOI:** 10.1002/adem.200400129
4. Kumar, S.; Chakraborty, M.; Sarma, S.; Murty, B.S. *J. Wear* **2008**, *265*, 134. **DOI:** 10.1016/j.wear.2007.09.007
5. Emamy, M.; Mahta, M.; Rasizadeh, J. *J. Composites Sci. Tech*. **2006**, *66*, 1063. **DOI:** 10.1016/j.compstech.2005.04.016
6. Yue, N. L.; Lu, L.; Lai, M.O. *J. Composite Structures* **1999**, *47*, 691. **DOI:** 10.1016/s0263-8223(00)00037-4
7. Ma, X.; Li, C.; Du, Z.; Zhang, W. *J. Alloys and Compounds*. **2004**, *370*, 149. **DOI:** 10.1016/j.jallcom.2003.09.017
8. Liang, Y.; Zhou, J.; Dong, S.; Tong, Y. *J. Wuhan Univ. of Tech. Mater. Sci. Ed*. **2008**, *23*, 342.
9. Fjellstedt, J.; Anders, E.W.; Jarfors. *J. Materials Sci. and Engg*. **2005**, A 413–414, 527. **DOI:** 10.1016/j.msea.2005.09.054
10. Degang, Zhao.; Xiangfa, Liu.; Yuxian, Liu.; Xiufang, B. *J. Materials Science* **2005**, *40*, 4365. **DOI:** 10.1007/s10853-005-0796-3
11. Tu , J.P.; Wang, N.Y.; Yang, Y.Z.; *J. Materials Letters* **2002**, *52*, 448. **DOI:** 10.1016/s0167-577x(01)00442-6
12. Fjellstedt, J.;Anders E.W.; Jarfors.; Svendsen, L. *J. Alloys and Compounds*, **1999**, 283, 192. **DOI:** 10.1016/s0925-8388(98)00892-5